$C_{(sp3)}$–H Oxidative Addition at Tantalocene Hydrides

Steven M. Rehbein, Matthew J. Kania, and Sharon R. Neufeldt*

Department of Chemistry and Biochemistry, Montana State University, Bozeman, MT 59717, United States

ABSTRACT: Although late transition metals are well-known to activate alkane C—H bonds through oxidative addition, this mechanistic step is atypical for early transition metals. Instead, prior examples of intermolecular $C_{(sp3)}$—H activation at early transition metals tend to proceed through σ-bond metathesis or 1,2-addition mechanisms. Recent theoretical work suggested that tantalocenes may be capable of activating aliphatic C—H bonds by oxidative addition. Herein, we demonstrate that mono-alkyl-substituted tantalocenes $^{R}Cp_2TaH_3$ undergo H/D exchange on the alkyl substituent "R" in the presence of C_6D_6, indicating that intramolecular $C_{(sp3)}$—H activation takes place. Moreover, Cp_2TaH_3 was found to catalyze H/D exchange between H_2 and octane-d_{18} and methylcyclohexane-d_{14}, representing involvement of an intermolecular $C_{(sp3)}$—H activation step. DFT calculations support $C_{(sp3)}$—H oxidative addition at transient Ta(III), a mechanistic step that has not been previously seen for intermolecular activation of alkanes at tantalum.

INTRODUCTION

Despite nearly a century of research, hydrocarbon activation remains largely an unfulfilled promise of molecular C—H activation catalysts.[1] A key challenge to achieving this goal is the fundamentally low reactivity of $C_{(sp3)}$—H bonds. The majority of research into molecular catalysts for C—H activation has focused on late transition metals. Early metals are less studied, in large part due to the inherent challenges of handling them, such as their high oxophilicity[2] and reactivity. However, because of their electropositivity, low-valent early transition metals can be especially reactive toward inert bonds.[3] Moreover, early metals are known to participate in reaction steps such as σ-bond metathesis[4] that are uncommon with late metals, suggesting the possibility of combining C—H activation with other unusual elementary steps to form novel catalytic manifolds. Because of these properties, the use of early transition metals for C—H activation remains an important area of study.

There exist several examples of *intra*molecular cleavage of unactivated $C_{(sp3)}$—H bonds at early transition metals,[5,6] including examples that likely proceed through an oxidative addition mechanism.[6] However, in cases of *inter*molecular activation of aliphatic C—H bonds promoted by early transition metals, C—H cleavage tends to take place through a σ-bond metathesis or related mechanism[7,8] or through 1,2-addition across metal-ligand multiple bonds.[9,10] In these reactions, there is no change to the oxidation state of the high-valent (typically d^0) metal. However, recent computational studies in our group hinted that tantalocenes may be capable of activating aliphatic C—H bonds through an oxidative addition pathway.[11] Herein we describe experimental studies, together with additional computational work, demonstrating that tantalocene hydrides can activate $C_{(sp3)}$—H bonds in both an intra- and intermolecular fashion.

RESULTS AND DISCUSSION

Overview. We previously explored the rate of H/D exchange between deuterated aromatic solvents and Cp_2TaH_3, $CpCp^*TaH_3$, and $Cp^*_2TaH_3$ ($Cp^* = \eta^5$-C_5Me_5). These studies indicated that Cp_2TaH_3 is much more active than the complexes containing the permethylated ligand, but that it is also more prone to decomposition under the high temperatures needed for C—H activation. Consequently, we speculated that analogues of Cp_2TaH_3 bearing monosubstituted Cp ligands might provide a better balance between reactivity and stability. A series of Ta(V) trihydrides with monoalkylated Cp ligands was prepared through modification of previously described syntheses (Figure 1).[12,13] In the process of analyzing these complexes' reactivity toward intermolecular H/D exchange with C_6D_6, we found evidence for intramolecular $C_{(sp3)}$—H activation, as described below. Further experimental studies demonstrated that Cp_2TaH_3 is also competent at activating $C_{(sp3)}$—H bonds in an intermolecular fashion, as had been suggested by DFT calculations.

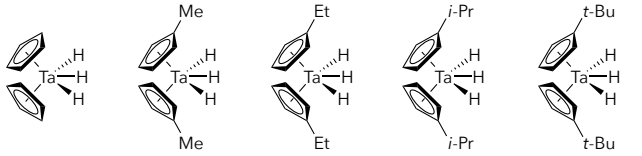

Cp_2TaH_3 (**1**) $^{Me}Cp_2TaH_3$ (**2**) $^{Et}Cp_2TaH_3$ (**3**) $^{iPr}Cp_2TaH_3$ (**4**) $^{tBu}Cp_2TaH_3$ (**5**)

Figure 1. Tantalocenes examined in this work.

H/D Exchange Between Aromatic Solvent and Ta(V) Hydrides Bearing Monoalkylated Cp Rings. Each complex shown in Figure 1 was subjected to heating at 100 °C in benzene-d_6 (Table 1). Under these conditions, tantalocenes are known to effect H/D exchange between the metal and the deuterated solvent, leading to replacement of the tantalum hydrides with deuterium.[11,14,15] We tracked the rates of H/D exchange by monitoring disappearance of the hydride signals by ^{1}H NMR relative to an internal standard (cyclohexane). Furthermore, when a hydride on tantalum is replaced with deuteride, changes to the splitting pattern of the neighboring hydrides are observable,[14] and these changes served as qualitative verification that the decreased integration of the hydride signals is due, at least in part, to H/D exchange rather than some other type of decomposition.

Under our experimental conditions, benzene-d_6 is in excess (benzene-d_6:Ta ≈ 500:1), such that the rate of H/D exchange between tantalum and solvent is expected to follow pseudo first order kinetics (Eq 1):

$$-\frac{d[\mathrm{Ta}]}{dt} = k[\mathrm{Ta}] \qquad \text{(Eq 1)}$$

As such, we report the rates of H/D exchange in terms of a first order rate constant k, obtained from a least squares regression of a linear plot of ln([Ta]) vs. time (see SI). A complicating factor in analyzing H/D exchange rates in this manner is that the tantalum hydride signals could also decrease for reasons not related to deuteration (*i.e.*, decomposition).[16] To account for this possibility, we also measured the (much smaller) rates of disappearance of the aromatic ^{R}Cp signals. Assuming that the ^{R}Cp ligand does not undergo deuteration, any decrease in the aromatic signal(s) would correspond to catalyst decomposition, and this information could be used to correct the rate of H/D exchange on tantalum to account for decomposition (see SI for details).

In Table 1, the measured rate of decomposition (disappearance of aromatic ligand signals) is denoted k_{decomp}, and the uncorrected rate of H/D exchange (disappearance of Ta—H signals) is denoted k_{obs}. The "corrected" rate constant for H/D exchange, denoted k_{corr}, is derived as $k_{\mathrm{corr}} = k_{\mathrm{obs}} - k_{\mathrm{decomp}}$. Finally, relative rate constants based on k_{corr} are provided as k_{rel}. It is worth noting that later studies indicate that H/D exchange may occur on the aromatic positions of the ^{R}Cp ligand (*vide infra*), potentially complicating the interpretation of "k_{decomp}". However, because k_{decomp} is quite small relative to k_{obs}, its impact on k_{rel} is negligible.

Table 1. Rate Constants for Decomposition of ^{R}Cp$_2$TaH$_3$ and H/D Exchange Between Tantalum Hydrides and Benzene-d_6 at 100 °C [a]

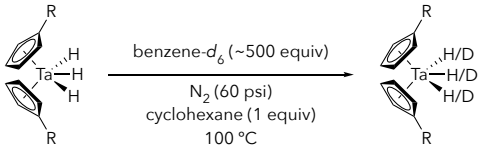

complex	R	k_{decomp}	k_{obs}	k_{corr}	k_{rel}
1	H	2.9(2)	47(6)	44(6)	1.0
2	Me	1.48(4)	61(3)	59(3)	1.3
3	Et	1.1(1)	45(5)	44(5)	1.0
4	*i*-Pr	1.12(8)	24(8)	23(8)	0.5
5	*t*-Bu	0.90(1)	20(2)	19(2)	0.4

[a] All experiments were performed in triplicate, and results are an average of the collected data. Standard error in the last significant figure is reported in parentheses. Reactions were followed for 6 h with heating at 100 °C under 60 psi N_2. Rate constants are reported in units of h^{-1} x 10^2, and k_{obs} was measured by monitoring the disappearance of hydride signals relative to cyclohexane. The decomposition rate constant k_{decomp} was obtained from disappearance of the aromatic ^{R}Cp signal(s) (for complexes **2**–**5**, the two aromatic signals were averaged).

The results of the experiments in Table 1 show that all five complexes catalyze H/D exchange with benzene-d_6 at similar rates. All of the alkylated complexes showed slower disappearance of the ^{R}Cp signals ("decomposition") than Cp_2TaH_3.

We undertook DFT calculations to analyze the energetics of benzene activation by these complexes (Table 2). The DFT method (see Table caption and SI for details) was chosen based on benchmarking reported in our previous study of the reaction of Cp_2TaH_3 with arenes.[11] An oxidative addition mechanism was calculated, as previously reported. [11] This mechanism involves initial loss of H_2 from ^{R}Cp$_2$TaH$_3$ to generate a high-energy Ta(III) monohydride **A**. The monohydride forms a π-complex with benzene (**B**) and then oxidatively adds into a benzene C—H bond. The lowest energy transition state for C—H activation is **TSC**, leading to **D** in which the aryl group is in the central position on tantalum and the nascent hydride is in a lateral position. However, it is likely that **D** and its configurational isomer (with Ph in a lateral position) are in equilibrium at high temperatures.[17] The configurational isomer of **D** could lose HD if the reaction takes place in deuterated benzene, thus explaining the previously reported observation of HD in the headspace of this reaction.[14a,b,c,e]

The DFT calculations predict a different reactivity order than observed experimentally. Experimentally, the rate of H/D exchange at ^{R}Cp$_2$TaH$_3$ follows the order: Me > Et ≈ H > *i*-Pr ≈ *t*-Bu. DFT predicts the order: *t*-Bu > Me > H > *i*-Pr > Et. However, the predicted free energy barriers to C—H activation are all within 1.5 kcal/mol of each other. Furthermore, the range of experimental rate constants (k_{corr}) correspond to reaction barriers that are within 0.9 kcal/mol of each other, so the discrepancy between theory and experiment is

within reasonable error for DFT calculations. Nevertheless, because the close structural similarity of the calculated transition states should lead to minimal error in their relative energy values, we suspected that there might be another explanation for the subtle mismatch between theory and experiment. In particular, we considered that C—H activation of the alkyl substituents on the Cp rings could occur in competition with solvent activation, affecting the observed rates of H/D exchange at Ta. However, only very slight changes to the alkyl signal integrations and shapes were detected in the ^{1}H NMR spectra for the experiments in Table 1, so the existence of H/D exchange activity at the alkyl substituents was inconclusive at this temperature (100 °C).

Table 2. Energetics of Benzene Activation at Cp_2TaH_3 Derivatives Predicted by DFT Calculations[a]

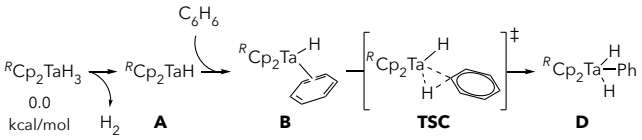

		ΔG (kcal/mol)			
complex	R	**A**	**B**	TSC	**D**
1	H	21.9	18.4	30.5	16.2
2	Me	20.5	17.1	30.5	16.2
3	Et	22.4	17.7	31.4	15.3
4	*i*-Pr	21.0	18.7	31.4	15.6
5	*t*-Bu	23.3	18.8	30.0	13.9

[a]Calculations were performed at the CPCM(benzene)-M06/6-311++G(2d,p)/SDD(Ta)/MO6L/6-31+G(d,p)/LANL2DZ(Ta) level of theory. Free energy values in kcal/mol are corrected for concentration ([Ta] and [H_2] = 0.022 *M*, [PhH] = 11.0 *M*). Thermochemical corrections were carried out at 373.15 K using the GoodVibes code.[18]

Intramolecular C—H Activation. We undertook additional DFT calculations to investigate the possibility of intramolecular C—H activation of the alkyl-substituted ^{R}Cp$_2$TaH$_3$ complexes. Scheme 1 illustrates the results with ^{Me}Cp$_2$TaH$_3$ (see SI for results with the other complexes). For this complex, intramolecular C—H activation is calculated to have a barrier about 1.3 kcal/mol lower than intermolecular activation of benzene, when concentrations are not considered (i.e., when all structures are assumed to be at a standard pressure of 1 atm, data not shown). Correcting for the high concentration of benzene as a solvent (11.0 *M*) relative to Ta (0.022 *M*) lowers the energy of **TS2C** by about 4.6 kcal/mol to +30.5 kcal/mol. Nevertheless, intramolecular C—H activation is likely to be competitive with benzene activation.

Scheme 1. Comparison of the Calculated Pathways for the Intermolecular Reaction of ^{Me}Cp$_2$TaH$_3$ with Benzene (Black) or Intramolecular C—H Activation (Blue).

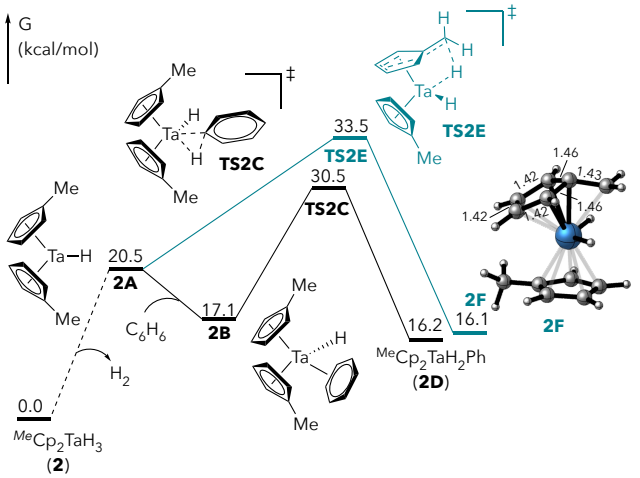

CPCM(benzene)-M06/6-311++G(2d,p)/SDD(Ta)//M06L/6-31+G(d,p)/LANL2DZ(Ta)
Energy values are corrected for concentration ([Ta] and [H_2] = 0.022 *M*, [PhH] = 11.0 *M*).
Thermochemical corrections were carried out at 373.15 K.

The structure resulting from intramolecular activation of ^{Me}Cp$_2$TaH$_3$ (**2F**) can be described as a "tuck-in" complex.[19] Its geometry is consistent with a hybrid between η^5,η^1 binding and fulvene-like η^4,η^2 binding. There is some pyramidalization of the exo-methylene, as would be expected for an η^5,η^1 geometry, but the bond lengths in the Cp ring are diene-like. The fulvene binding character is consistent with previous NMR analysis of related tuck-in complexes of pentamethylcyclopentadienyl tantalum species.[20]

For ^{Et}Cp$_2$TaH$_3$ (**3**) and ^{iPr}Cp$_2$TaH$_3$ (**4**), intramolecular activation of the 2° and 3° α-C—H bonds via **TSE** is predicted to be slightly faster than activation of the 1° β-C—H bonds via **TSF** (Table 3). However, the barriers to activation of all of the alkyl C—H bonds of complexes **2**-**5** are very similar. Taken together, these calculations suggest that intramolecular C—H activation is likely competitive with H/D exchange with benzene for all of the monosubstituted ^{R}Cp$_2$TaH$_3$ complexes. If this is true, then we expected that intramolecular H/D exchange should be detectable experimentally.

Table 3. Energetics of Intramolecular C—H Activation at Cp_2TaH_3 Derivatives Predicted by DFT Calculations[a]

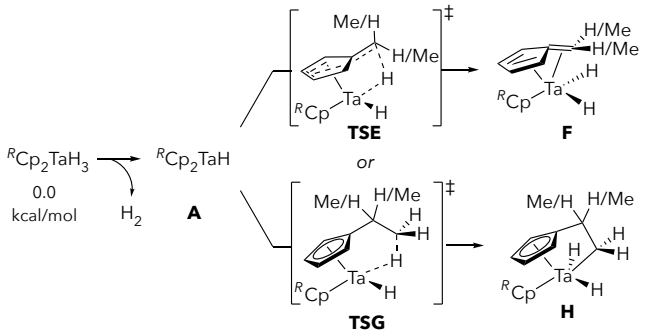

		ΔG (kcal/mol)			
complex	R	TSE	**F**	TSG	**H**
2	Me	33.5	16.1	--	--
3	Et	33.6	16.7	34.6	23.2
4	*i*-Pr	33.7	18.3	34.5	22.8
5	*t*-Bu	--	--	33.1	21.6

[a]Calculations were performed at the CPCM(benzene)-M06/6-311++G(2d,p)/SDD(Ta)/MO6L/6-31+G(d,p)/LANL2DZ(Ta) level of theory. Free energy values in kcal/mol are corrected for concentration ([Ta] and $[H_2]$ = 0.022 *M*). Thermochemical corrections were carried out at 373.15 K using the GoodVibes code.[18]

In an effort to observe these intramolecular processes experimentally, we repeated the experiments heating $^{R}Cp_2TaH_3$ in C_6D_6 at a higher temperature of 120 °C under 60 psi of N_2 (Table 4). Indeed, under these conditions, it became clear that intramolecular H/D exchange takes place on the alkyl substituents, based on the decreased integrations of the corresponding signals relative to the aromatic ^{R}Cp signals and relative to internal standard. Table 4 provides the observed rate constants for disappearance of the signals corresponding to each of the C—H bonds in the complexes. At this higher temperature, we also observed evidence for H/D exchange on the ^{R}Cp backbone itself (i.e., a change in the ratio of the two signals on ^{R}Cp). As such, erosion of the aromatic signals relative to the internal standard is not a good proxy for unproductive decomposition, and so the rate constants in Table 4 are uncorrected for decomposition.

Table 4. Rate Constants for H/D Exchange Between Benzene-d_6 and All Sites of $^{R}Cp_2TaH_3$ at 120 °C[a]

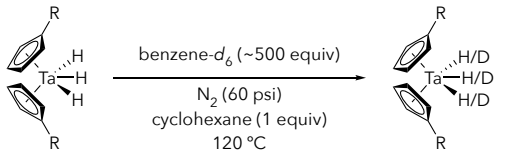

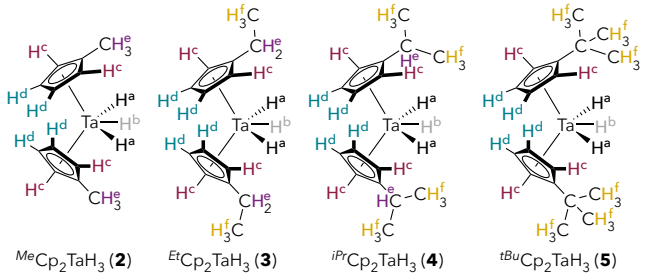

entry	R	position	k_{obs}	k_{rel}	$k_{rel\text{-}adj}$[b]
1	Me	a + b	53(5)	25.4	17.0
2		c	5.5(1)	2.6	2.6
3		d	10.4(8)	5.0	5.0
4		e	6.6(7)	3.1	2.1
5	Et	a + b	42.1(7)	20.3	13.5
6		c	4.2(3)	2.0	2.0
7		d	10(1)	4.8	4.8
8		e	15(3)	7.4	7.4
9		f	2.6(4)	1.3	0.8
10	*i*-Pr	a + b	42(1)	20.1	13.4
11		c	3.1(2)	1.5	1.5
12		d	7(1)	3.6	3.6
13		e	10(2)	4.8	9.7
14		f	8(1)	3.6	1.2
15	*t*-Bu	a + b	38(2)	18.4	12.2
16		c	2.08(3)	1.0	1.0
17		d	6(1)	2.8	2.8
18		f	24(4)	11.6	2.6

[a] All experiments were performed in triplicate, and results are an average of the collected data. Standard error in the last significant figure is reported in parentheses. Reactions were followed for 6 h with heating at 120 °C under 60 psi N_2. Rate constants are reported in units of h^{-1} x 10^2. k_{rel} is reported relative to the slowest rate in the table (entry 16). [b]Adjusted for statistical probability (i.e., k_{obs} was divided by the number of protons at the indicated site before calculating $k_{rel\text{-}adj}$).

The experimental results show some qualitative correlations to the DFT calculations. For $^{Et}Cp_2TaH_3$ and $^{iPr}Cp_2TaH_3$, H/D exchange is faster at the α-C—H (position "e") than at the β methyls ("f"). The highest rate of intramolecular H/D exchange on carbon was observed at the 3° α-C—H bond ("e") of $^{iPr}Cp_2TaH_3$.

The rate of erosion of the aromatic signals of $^{Me}Cp_2TaH_3$ and $^{Et}Cp_2TaH_3$ ("c" and "d") is slower or comparable to the

rate of erosion (H/D exchange) of the alkyl signals. Some of the disappearance of the Cp signals could be due to decomposition pathways. However, the unequal rate of disappearance of "c" and "d" indicates that the Cp ring itself becomes deuterated, likely through intermolecular pathways.[14a] The C—H bonds distal to the alkyl substituent ("d") appear to be more reactive toward H/D exchange, which is likely due to sterics. Indeed, the highest selectivity for H/D exchange at the distal bonds of ^{R}Cp is seen when R = *t*-Bu [H^d/H^c = 2.8 (entries 16-17)].

Intermolecular Alkane C—H Activation. Inspired by the evidence for intramolecular $C_{(sp3)}$—H activation, we conducted DFT calculations on the reaction of the unsubstituted complex Cp_2TaH_3 with alkanes (Table 5). This complex cannot undergo competing intramolecular C—H activation, and we expected that in the absence of aromatic solvents [which can π-complex to transient Ta(III)], alkane activation might be feasible. Analogous to the activation of arenes, an oxidative addition mechanism via **1A** was calculated for activation of hydrocarbons. An alternative σ-bond metathesis mechanism for C—H activation of methane was also considered, but this pathway is prohibitively high-energy, apparently due to steric crowding around Cp_2TaH_3 (see SI).

Table 5. Energetics of Intermolecular C—H Activation at Cp_2TaH_3 Predicted by DFT Calculations[a]

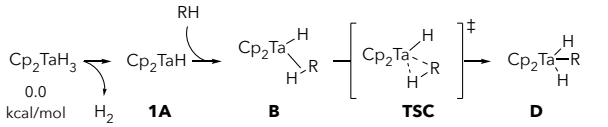

entry	C—H bond	**B** (ΔG, kcal/mol)	**TSC** (ΔG‡, kcal/mol)
1[b]	Ph**H**	18.4	30.5
2	PhC**H**$_3$	28.3	33.5
3	C**H**$_4$	26.4	33.2
4	C**H**$_3$(CH$_2$)$_2$	27.4	34.4
5	(CH$_3$)$_2$C**H**$_2$	26.2	39.5
6	(CH$_3$)$_3$C**H**	27.4	42.3

[a]Calculations were performed at the CPCM(solvent)-M06/6-311++G(2d,p)/SDD(Ta)/ M06L/6-31+G(d,p)/LANL2DZ(Ta) level of theory using benzene (entry 1), toluene (entry 2), or cyclohexane (entries 3-6). Free energy values in kcal/mol are corrected for concentration ([Ta] and [H_2] = 0.022 *M* for entry 1 and 0.019 M for entries 2-6, [PhH] = 11.0 *M*, [PhCH$_3$] = 9.41 *M*, and the concentration of the substrates in entries 3-6 was approximated as that of cyclohexane (9.26 *M*)). Thermochemical corrections were carried out at 373.15 K using the GoodVibes code.[18] [b]The structure of **B** when RH = PhH is a π complex rather than a σ-complex.

The calculations indicate that the barrier to activation of aliphatic 1° C—H bonds is about 4 kcal/mol higher than the barrier to activating an aromatic C—H bond of benzene (compare entries 3 and 4 to entry 1). Activating 2° and 3° C—H bonds appears significantly more difficult (entries 5-6). Thus, alkane activation at Cp_2TaH_3 should be more challenging than arene activation, but, at least for 1° C—H bonds, not necessarily prohibitively so.

We next conducted several experiments to evaluate the behavior of Cp_2TaH_3 toward activation of aliphatic C—H bonds. In preliminary experiments, deuterated solvent [cyclohexane-d_{12} or *n*-octane-d_{18}] was heated to 120 ºC together with Cp_2TaH_3 under an atmosphere of N_2 (60 psi) in an NMR tube for 24 h. Gratifyingly, H/D exchange was observed on tantalum in octane-d_{18}, a substrate that contains 1° C—H bonds, confirming for the first time that tantalocene hydrides can activate $C_{(sp3)}$—H bonds in an intermolecular fashion (Scheme 2A). Surprisingly, despite the higher barriers predicted for activation of 2° C—H bonds, the ^{1}H NMR spectrum for the reaction in cyclohexane-d_{12} also showed evidence for a small amount of H/D exchange at tantalum (Scheme 2B). This suggests that tantalum hydrides are competent (albeit inefficient) catalysts for C—H activation of 2° C—H bonds. Furthermore, this experimental observation indicates that the calculated barriers to C—H activation are somewhat overestimated. The artificially high predicted energies are likely due to underestimation of the entropy of H_2 that is generated together with Cp_2TaH (**1A** in Tables 2 and 5). The concentration of H_2 is treated as the same value as the concentration of **1A**, because these species are formed in equimolar amounts, but due to the low solubility of gaseous H_2, this concentration is certainly an overestimate. This error is propagated across all subsequent stationary points.

Scheme 2. Cp_2TaH_3 Becomes Partially Deuterated Upon Heating in Deuterated Alkane Solvents (A) d_{18}-Octane or (B) d_{12}-Cyclohexane

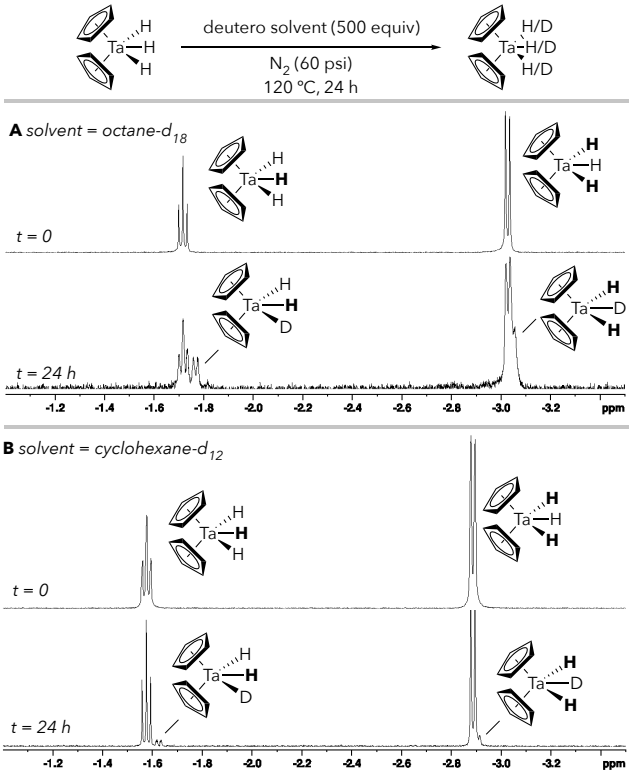

Because of the low concentration of tantalum, and thus the low availability of ^{1}H for incorporation into the deuteroalkanes (i.e., ^{1}H from Cp_2TaH_3), it was not possible to determine the site selectivity of H/D exchange on *n*-octane.

To investigate selectivity, we turned to running reactions of *n*-octane-d_{18} (b.p. = 126 °C) or methylcyclohexane-d_{14} (b.p. = 101 °C), under an atmosphere of H_2 with heating to near the solvent boiling point. Under these conditions, Ta could catalyze H/D exchange between H_2 and deuteroalkane, potentially leading to a measurable amount of hydrogen incorporation into the deuteroalkane. The reactions were run in pressure vessels with a large headspace, rather than in an NMR tube, to enable pressurization with higher molar equivalents of H_2 (~5 atm of H_2 ≈ 1 equiv of H_2 relative to alkane). The reactions were heated to 120 °C (octane) or 100 °C (methylcyclohexane) for 48 h, and then the residual solvent signals were analyzed by ^{1}H NMR. Cyclohexane (C_6H_{12}) was used as an internal standard in these experiments. Because of the low concentration of standard, and considering the minimal H/D exchange observed between Ta and cyclohexane-d_{12} in Scheme 2B, deuteration of the cyclohexane internal standard in the experiments shown in Scheme 3 is expected to be negligible. However, we cannot rule out that deuteration of the internal standard could inflate the apparent "yields" of protio-octane or methylcyclohexane, and as such the change in solvent signal *ratios* is a more meaningful indication of H/D exchange than the absolute change in signal integrations.

For both *n*-octane-d_{18} and methylcyclohexane-d_{14}, the residual protic solvent signals grew after 48 h, indicating exchange between solvent and H_2. Importantly, the ratio of residual solvent signals also changed, demonstrating different extents of H/D exchange at the different sites. With *n*-octane, the methyl signal grew slightly more than the methylene signals, suggesting a slightly greater extent of H/D exchange at the 1° carbons compared to the 2° positions (Scheme 3A). For methylcyclohexane, an interesting pattern of residual solvent signal growth emerged, ranging from 39-83% and corresponding to different isotopomers of $C_7D_{13}H$ (Scheme 3B). For the axial hydrogens, larger signal growth was seen for the positions closer to the methyl substituent compared to the more distal positions (b > d > e > g). The methyl signal itself showed intermediate growth (a, 47%), but not all H/D exchange at this position may be captured by the integration of the signal labeled as "a" since the signal for its isotopologue ($C_7D_{12}H_2$, with an H at both the methyl at at the 3º position) would be shifted slightly downfield. The significant H/D exchange at C1 ("b") was initially surprising because the calculations suggest that a 3° C—H bond should be very challenging to activate compared to 1° and even 2° bonds. Somewhat less H/D exchange was seen overall at the equatorial positions, and the least signal growth was observed at the most distal site (h, 39%). Additionally, a new signal emerged slightly downfield of "d", likely corresponding to an isotopologue(s) (i.e., $C_7D_{12}H_2$).

Scheme 3. Growth of Deuterated Solvent Signals Indicates H/D Exchange Between H_2 and (A) d_{18}-Octane or (b) d_{14}-Methylcyclohexane

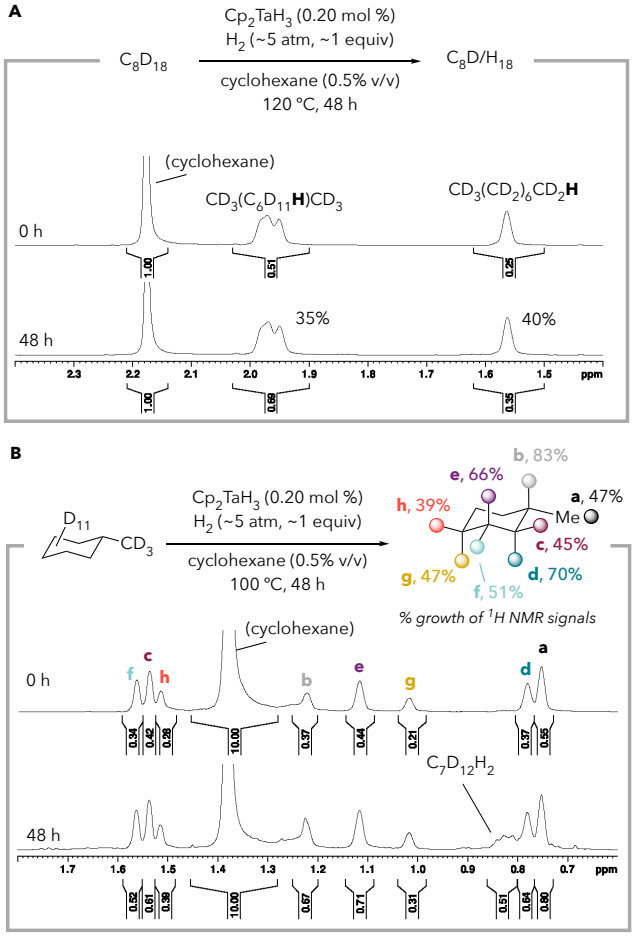

Explanation for H/D Exchange at Hindered Sites. The calculations indicate that the barrier to C—H activation of a 3° C—H bond is at least 7 kcal/mol higher than the barrier to activating a 1° C—H bond (Table 5). Nevertheless, the 3° position of deuterated methylcyclohexane showed extensive H/D exchange experimentally (Scheme 3B). Furthermore, H/D exchange at most of the 2° positions of methylcyclohexane was on par with the amount of H/D exchange at the 1° position. This observation apparently contradicts the calculated prediction that 2° C—H bonds should be more challenging to activate than 1° C—H bonds (by about 4-5 kcal/mol, Table 5). Furthermore, the considerable extent of H/D exchange at most of the 2° positions of methylcyclohexane seems inconsistent with the only very subtle evidence for H/D exchange at tantalum in the reaction with d_{12}-cyclohexane, which contains only 2° C—H bonds (Scheme 2B).

Consequently, we considered the possibility that C—H activation takes place primarily (or exclusively) at the methyl position of methylcyclohexane, and H/D exchange at the other sites is the result of β-hydride elimination/reinsertion. DFT calculations on a model substrate (isobutane) indicate that the proposed pathway is feasible (Scheme 4). C—H activation at the 1° position of isobutane can lead to intermediate **6I** in which the alkyl group is in a lateral

position on tantalum (contrast to **6D**, in which carbon is in the central position). Although the transition structure **TS6Ci** that leads directly to **6I** is higher than the one leading to its configurational isomer **6D**, it is likely that **6D** and **6I** can thermally interconvert.[17] Intermediate **6I** can reductively eliminate dihydrogen to give the high-energy Ta(III) intermediate **6J**, which undergoes an exergonic β-hydride elimination through a transition state **TS6K** that is calculated to have a similar energy to the 1° C—H activation transition structure (**TS6ii**). Importantly, **TS6K** is lower than the predicted barrier to activation of a 2° C—H bond (Table 5, entry 5). Based on the feasibility of **TS6K**, it is likely that the large extent of H/D exchange observed at the 3° position of methylcyclohexane (Scheme 3B) results from initial activation of a 1° C—D bond followed by β-deuteride elimination of the 3° C—D and reinsertion of H_2.

Scheme 4. Calculated Pathway for C—H Activation Followed by β-Hydride Elimination for a Model Alkane.

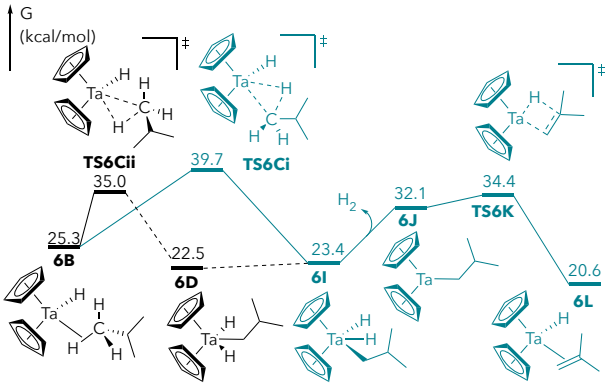

CPCM(cyclohexane)-M06/6-311++G(2d,p)/SDD(Ta)//M06L/6-31+G(d,p)/LANL2DZ(Ta)
Energy values are corrected for concentration ([Ta] and [H_2] = 0.019 *M*, [isobutane] = 9.26 *M*) and are reported relative to separated reactants (**1** + isobutane, ΔG = 0.0 kcal/mol).
Thermochemical corrections were carried out at 373.15 K.

CONCLUSION

Mono-alkyl-substituted complexes $^{R}Cp_2TaH_3$ are shown to undergo H/D exchange with benzene-d_6, leading to deuterium incorporation on tantalum as well as on the alkyl substituent "R" and the aromatic positions of the ^{R}Cp ligand. The H/D exchange with benzene was previously shown to proceed most likely through initial reductive elimination of H_2 to generate Ta(III), which undergoes oxidative addition into a Ph—H bond. DFT calculations indicate an analogous pathway for intramolecular activation of $C_{(sp3)}$—H bonds of $^{R}Cp_2TaH_3$. Based on the observation that the tantalum of $^{R}Cp_2TaH_3$ can intramolecularly activate $C_{(sp3)}$—H bonds, the intermolecular reactivity of Cp_2TaH_3 toward alkanes was examined. H/D exchange was detectable between Cp_2TaH_3 and deuterated octane and cyclohexane under thermal conditions. Moreover, Cp_2TaH_3 was found to catalyze H/D exchange between H_2 and octane-d_{18} and methylcyclohexane-d_{14}. Although DFT calculations suggest a strong steric bias toward activation of 1° C—H bonds, in practice the H/D exchange catalyzed by Cp_2TaH_3 is somewhat indiscriminate. H/D exchange with cyclohexane-d_{12}—containing only 2° C—H bonds—was minimal, but extensive H/D exchange at most positions of methylcyclohexane-d_{14} (including 2° and 3° carbons) is observed. The 1° methyl group may serve as an "onramp" for tantalum to catalyze H/D exchange at the other sites: initial C—H activation at the 1° position can be followed by β-hydride elimination/reinsertion to scramble the isotopes at the other sites.

DFT calculations suggest that activation of alkanes proceeds through an analogous pathway to activation of arenes, involving oxidative addition at transient Ta(III). Although activation of $C_{(sp3)}$—H bonds by oxidative addition at late transition metals is well established, this mechanism is unusual for activation of hydrocarbons at early transition metals. In prior reports, intermolecular activation of alkanes at early transition metals proceeds through alternative mechanisms (1,2-addition or σ-bond metathesis).[7,8,9] The atypical mechanism employed by the tantalocene in this study can be attributed to its structure. Cp_2TaH_3 does not have any metal-ligand multiple bonds (a prerequisite for 1,2-addition of a C—H bond), and σ-bond metathesis between Cp_2TaH_3 and a C—H bond is prohibitively high-energy, apparently due to sterics. However, H_2 is easily lost from Cp_2TaH_3 upon heating (DFT computes this step to be "barrierless"[11]), and the resulting low-valent Ta(III) complex is much more reactive than the parent Ta(V) complex due to its high-energy d-electrons, open coordination sites, and decreased steric hindrance.

There is growing recognition that catalysis by low-valent early transition metals has potential for unlocking novel transformations.[3] The work reported herein suggests that intermolecular $C_{(sp3)}$—H oxidative addition is another elementary step that should be considered in the repertoire of low-valent early transition metals.

EXPERIMENTAL SECTION

General Materials and Methods.

Lithium aluminum hydride, dimethyldicyclopentadiene, *n*-hexadecane, pyridine, and *tert*-butylamine were obtained from Acros Organics and used as received. Pyrrolidine and sodium bis(2-methoxyethoxy)aluminum hydride (70% w/w in toluene) were obtained from Acros organics in ACROSeal bottles and used as received. Dicyclopentadiene was obtained from Acros Organics and passed across a short silica plug to remove water and stabilizer prior to use. Sodium metal (foil-wrapped sticks in mineral oil) was obtained from Acros Organics and washed with copious hexanes prior to use. Sodium hydride (60% w/w dispersion in mineral oil) was obtained from Acros Organics and washed under airfree conditions with copious pentane prior to use. $TaCl_5$ was obtained from Acros Organics and purified by sublimation prior to use. Sodium metasilicate (anhydrous) was obtained from Alfa Aesar and used as received. Isotopically labeled compounds (benzene-d_6, $CDCl_3$, DMSO-d_6, cyclohexane-d_{12}, methylcyclohexane-d_{12}, octane-d_{18}) were obtained from Cambridge Isotopes and degassed and stored over 3 Å molecular sieves. Acetic acid, acetone, magnesium sulfate (anhydrous), methanol, sodium bicarbonate, and sodium chloride were obtained from Fisher Chemical and used as received. Dichloromethane, diethyl ether, *n*-hexane, pentanes, tetrahydrofuran (THF), and toluene were obtained from Fisher Chemical and degassed and dried on a JC Meyer solvent system prior to use. Tri-*n*-butyltin chloride was obtained from Oakwood Chemical and used as received. Diethyldicyclopentadiene was obtained from Sigma-Aldrich and used as received. Methyl lithium (1.6 *M* in Et_2O) and *n*-butyl lithum (2.5 *M* in hexanes) were obtained from Sigma-Aldrich in Sure/Seal bottles and used as received. Cp_2TaH_3 (**1**) was prepared according to a literature procedure.[11] Unless otherwise noted, all operations were performed in a nitrogen-filled glovebox or using airfree techniques in oven-dried glassware. NMR spectra

were recorded at 298 K on a Bruker DRX 500 MHz (500.233 MHz for ^{1}H, 125.795 MHz for ^{13}C) spectrometer. Elevated-pressure ^{1}H NMR experiments were performed in 9-inch Wilmad Glass medium-walled high-pressure precision NMR tubes. ^{1}H and ^{13}C NMR chemical shifts are reported in parts per million (ppm) relative to TMS, with the residual solvent peak used as an internal reference [^{1}H: $CHCl_3$ (7.26 ppm), C_6D_5H (7.16 ppm), or DMSO-d_5 (2.50 ppm); ^{13}C: $CDCl_3$ (77.16 ppm), C_6D_6 (128.06 ppm), or DMSO-d_6 (39.52 ppm)]. Multiplicities are reported as follows: singlet (s), doublet (d), triplet (t), quartet (q), sextet (sext), septet (sept), and multiplet or multiple overlapping signals (m).

General Procedure for Measuring H/D Exchange Rates by ^{1}H NMR (Reactions in NMR Tube; Table 1; Table 4): In a 4 mL vial within a nitrogen-filled glovebox, $^{R}Cp_2TaH_3$ (freshly-sublimed, 0.2 mol % relative to substrate) was fully dissolved in a solution of deuterated benzene (1.80 mL) containing cyclohexane (0.2 mol % relative to benzene). The resulting solution was divided equally (0.60 mL each) into three medium-wall high-pressure precision NMR tubes (Wilmad, 9" length, 3.46 mm internal diameter) and the tubes were sealed with Teflon stopcocks and removed from the glovebox. One at a time, the tubes were connected to a Schlenk line and pressurized to 60 psi (4.14 bar) nitrogen. Initial ^{1}H NMR spectra (500 MHz, 32 scans, D1 relaxation delay = 10 s) were obtained of each sample (time = 0 h) and the samples were heated in a Chemglass NMR tube reaction heating block for a total of six hours (not including breaks for acquiring NMR spectra). NMR spectra were acquired approximately every hour (exact times were recorded and used during analysis of the results). During processing, the integration values of all signals were standardized relative to the cyclohexane signal (the cyclohexane signal integration was set to 10). Integration values were then normalized by multiplying the integral by a scalar value to correct for the actual initial concentrations at t = 0.

Procedure for H/D Exchange Reactions Between Deuterated Alkanes and Cp_2TaH_3 Under N_2 in NMR Tubes (Scheme 2): In a 4 mL vial within a nitrogen filled glovebox, Cp_2TaH_3 (**1**, freshly-sublimed, 0.20 mol % relative to alkane) was dissolved in deuterated alkane. The resulting solution was divided equally (0.60 mL each) into three medium-wall high-pressure precision NMR tubes (Wilmad, 9" length, 3.46 mm internal diameter, each containing a benzene-filled flame-sealed capillary tube as an internal standard) and the tubes were sealed with Teflon stopcocks and removed from the glovebox. One at a time, the tubes were connected to a Schlenk line and pressurized to 60 psi (4.14 bar) nitrogen. Initial ^{1}H NMR spectra (500 MHz, 32 scans, D1 relaxation delay = 10 s) were obtained of each sample (time = 0 h) and the samples were heated in a Chemglass NMR tube reaction heating block for a total of twenty-four hours, after which a final ^{1}H NMR spectrum was collected (t = 24 h).

Procedure for H/D Exchange Reactions under H_2 in Pressure Vessels (Scheme 3): Within a nitrogen-filled glovebox, Cp_2TaH_3 (freshly-sublimed, 0.20 mol % relative to alkane) was fully dissolved in a solution of deuterated alkane (~ 10 mmol—exact quantity chosen to achieve a 1:2 molar ratio of deutrated substrate to H_2 once pressurized) containing cyclohexane (1 mol % relative to substrate). The solution was divided between a glass pressure reaction vessel (Andrews Glass, 3 fl oz/89 mL volume) and a J. Young NMR tube (Wilmad, 5 mm OD). An initial ^{1}H NMR spectrum was immediately collected of the aliquot in the NMR tube (500 MHz, 32 scans, D1 relaxation delay = 10 s). The pressure vessel was sealed, removed from the glovebox, and cooled to -196 °C in liquid nitrogen. Once cooled, the vessel was evacuated and refilled to 1.0 atm H_2 (3x) and again sealed (note: although the pressure is 1 atm at 196 °C, it increases to 4.8 or 5.1 atm at 100 °C and 120 °C, respectively). The sealed vessel was allowed to warm to room temperature, then heated to 120 °C (*n*-octane-d_{18}) or 100 °C (methylcyclohexane-d_{14}) with stirring for 48 h. The vessel was again taken into a nitrogen-filled glovebox and the contents were transferred to a J. Young NMR tube and a final spectrum collected. During processing, the integration values of all signals were standardized relative to the cyclohexane signal.

Synthesis of Na[^{Me}Cp] (7): With cooling to 0 °C, methylcyclopentadiene monomer (7.61 g, 94.9 mmol, distilled twice through glass helices from the freshly-cracked monomer to eliminate cyclopentadiene contamination) was added to a mixture of sodium hydride (2.28 g, 94.9 mmol) in Et_2O and allowed to slowly warm to room temperature and stirred for 16 h. An arduous filtration under N_2 gave a solution that was concentrated to give a pale pink solid (2.07 g, 20.3 mmol, 21% yield). Spectral data are consistent with those previously reported.[21]

Synthesis of $Ta(=NCMe_3)Cl_3(Py)_2$ (8). The title compound was prepared according to a procedure adapted from the literature.[12d] *Tert*-butylamine (5.9 mL, 56 mmol) and pyridine (20.0 mL, 250 mmol) were added sequentially to a stirred heterogeneous mixture of freshly-sublimed $TaCl_5$ (10.00 g, 27.9 mmol) and Na_2SiO_3 (6.84 g, 56.0 mmol) in toluene (80 mL) and Et_2O (20 mL). The mixture was stirred for 18 h, after which it was filtered over Celite. The Celite plug was washed with toluene, and the combined filtrates were concentrated *in vacuo* to give an opaque yellow solid. Recrystallization from dichloromethane:pentane at –25 °C gave large yellow crystals after 5 days (8.04 g, 56% yield). Additional product can be obtained from the same recrystallization liquor with additional time and pentane additions. Spectral data are consistent with those previously reported.[12d]

Synthesis of $^{Me}Cp_2Ta(=NCMe_3)Cl$ (9): The title compound was prepared according to a procedure adapted from the literature for the analogous compound $Cp_2Ta(=NCMe_3)Cl$.[12c] With cooling to –84 °C, a solution of Na[^{Me}Cp] (**7**, 2.37 g, 23.2 mmol) in Et_2O (70 mL) and THF (17 mL) was added to a solution of $Ta(=NCMe_3)Cl_2(Py)_2$ (**8**, 5.17 g, 10.0 mmol) in Et_2O (340 mL) and the mixture was allowed to slowly warm to room temperature and stirred for 24 h. Solvent removal in vacuo gave a red oil that was extracted into pentane (3 x 100 mL), and concentration of the combined extracts gave a red solid (2.99 g, 6.7 mmol, 67% yield) that was used without further purification or characterization.

Synthesis of $^{Me}Cp_2TaH_3$ (2): The title compound was prepared according to a procedure adapted from the literature for the analogous compound Cp_2TaH_3.[12e] With cooling to –84 °C, a solution of $^{Me}Cp_2Ta(=NCMe_3)Cl$ (**9**, 2.99 g, 6.7 mmol) in Et_2O (65 mL) was added to a suspension of $LiAlH_4$ (1.03 g, 27.2 mmol) in Et_2O (65 mL) and the mixture was allowed to slowly warm to room temperature and stirred for 12 h. The mixture was cooled to 0 °C, and degassed, deionized water (2.0 mL, 111.0 mmol) was added dropwise. The mixture was allowed to warm slowly to room temperature and to stir until the suspension was free-flowing. Extraction into Et_2O (3 x 60 mL) and concentration of the combined extracts in vacuo gave an off-white solid (0.76 g, 2.2 mmol, 33% yield) showing ~1% contamination by (^{Me}Cp)$CpTaH_3$. ^{1}H NMR (500 MHz, C_6D_6, δ): 4.83 (t, *J* = 2.5 Hz, 4H), 4.69 (t, *J* = 2.5 Hz, 4H), 2.02 (s, 6H), -0.65 (t, *J* = 10.6 Hz, 1H), -2.21 (d, *J* = 10.6 Hz, 2H); ^{13}C NMR (126 MHz, C_6D_6, δ): 106.4, 88.1, 84.8, 16.3.

Synthesis of Na[^{Et}Cp] (10): Ethylcyclopentadiene dimer (3.77 g, 20.0 mmol) was added dropwise to a stirred suspension of sodium hydride (0.8690 g, 36.0 mmol) in hexadecane (40 mL) and heated at 195 °C for 16 h. After this time the mixture was allowed to cool to room temperature, and the product was collected via vacuum filtration, and washed with copious cold pentane to give a white solid (4.12 g, 35.5 mmol, 98 % yield) with an apparent ~6% remaining hexadecane impurity by ^{1}H NMR. Additional washing with pentane or *n*-hexane resulted in reduced yield without appreciable decrease in hexadecane impurity. ^{1}H NMR (500 MHz, DMSO-d_6, δ): 5.14 (t, *J* = 1.6 Hz, 4H), 2.41 (q, *J* = 7.5 Hz, 2H), 1.05 (t, *J* = 7.5 Hz, 3H). Note: this procedure differs significantly from that of the methyl analogue in that, here, the monomer is "cracked" in the presence of NaH in high-boiling hexadecane instead of prior to the addition of NaH. This modification was undertaken to avoid the difficulties associated with cracking and distilling small quantities of the expensive ethylcyclopentadiene dimer. The ethyl group,

however, dramatically increases the solubility of the sodium ^{R}Cp salt in hydrocarbon solvents and makes complete removal of hexadecane difficult.

Synthesis of ^{Et}Cp$_2$Ta(=NCMe$_3$)Cl (11): The title compound was prepared according to a procedure adapted from the literature for the analogous compound Cp$_2$Ta(=NCMe$_3$)Cl.[12c] With cooling to –84 °C, a solution of Na[^{Et}Cp] (2.74 g, 23.2 mmol) in Et$_2$O (70 mL) and THF (17 mL) was added to a mixture of Ta(=NCMe$_3$)Cl$_3$(Py)$_2$ (**8**, 5.16 g, 10.0 mmol) in Et$_2$O (340 mL) and the mixture was allowed to slowly warm to room temperature and stir for 16 h. After this time solvent was removed in vacuo to give a pasty solid that was extracted into pentane (3 x 50 mL). Concentration of the combined extracts gave a red oil (4.20 g, 8.9 mmol, 89% yield) that was used without further purification or characterization.

Synthesis of ^{Et}Cp$_2$TaH$_3$ (3): The title compound was prepared according to a procedure adapted from the literature for the analogous compound Cp$_2$TaH$_3$.[12e] With cooling to –84 °C, a solution of ^{Et}Cp$_2$Ta(=NCMe$_3$)Cl (**11**, 4.20 g, 8.9 mmol) in Et$_2$O (85 mL) was added to mixture of LiAlH$_4$ (1.36 g, 35.9 mmol) in Et$_2$O (85 mL) and the mixture was allowed to slowly warm to room temperature and stir for 16 h. After this time the mixture was cooled to 0 °C ,and degassed, deionized water (2.6 mL, 144.3 mmol) was added dropwise. The mixture was allowed to warm slowly to room temperature and to stir until the suspension was free-flowing. Extraction into Et$_2$O (2 x 80 mL) and concentration of the combined extracts gave a pale yellow solid with appreciable hexadecane contamination originating from Na[^{Et}Cp]. This contaminant co-distills alongside sublimation of ^{Et}Cp$_2$TaH$_3$, and so it was removed by a poor-yielding washing on silica gel with pentane followed by elution in Et$_2$O. Concentration of the Et$_2$O eluent gave of pale yellow solid (0.62 g, 1.68 mmol, 19% yield) in agreement with the expected structure by ^{1}H and ^{13}C NMR. ^{1}H NMR (500 MHz, C$_6$D$_6$, δ): 4.79 (t, *J* = 2.6 Hz, 4H), 4.71 (t, *J* = 2.6 Hz, 4H), 2.38 (q, *J* = 7.4 Hz, 4H), 1.06 (t, *J* = 7.4 Hz, 6H), -0.87 (t, *J* = 10.5 Hz, 1H), -2.42 (d, *J* = 10.5 Hz, 2H); ^{13}C NMR (126 MHz, C$_6$D$_6$, δ): 114.9, 85.7, 84.4, 23.8, 15.9.

Synthesis of 6,6'-dimethylfulvene (12): The title compound was prepared according to a procedure adapted from the literature.[22] Without the use of airfree techniques and with cooling to 0 °C, pyrrolidine (13.2 mL, 160.7 mmol) was added to a solution of cyclopentadiene (8.0 mL, 95.1 mmol, freshly "cracked" monomer) in acetone (6.0 mL, 81.0 mmol) and methanol (20 mL), giving an immediate color change from colorless to bright yellow. The mixture was allowed to warm to room temperature and stirred for 2 h, after which water (40 mL) and Et$_2$O (40 mL) were added and the mixture acidified (pH = 6.8) with acetic acid. The ethereal and aqueous phases were separated, and the aqueous phase was extracted into Et$_2$O (2 x 40 mL). The combined ethereal extracts were washed with saturated aqueous NaHCO$_3$ (4 x 40 mL), water (20 mL) and saturated aqueous NaCl (20 mL). The ethereal solution was dried with MgSO$_4$, filtered, and concentrated by rotary evaporation to give a bright yellow-orange liquid (7.80 g, 73.5 mmol, 77% yield). Spectral data are consistent with those previously reported.[22]

Synthesis of 5-(1-methylethyl)-1,3-cyclopentadiene (13): With cooling to 0 °C, a solution of 6,6'-dimethylfulvene (**12**, 6.37 g, 60.0 mmol) in Et$_2$O (75 mL) was added to a mixture of LiAlH$_4$ (1.14 g, 30.0 mmol) in Et$_2$O (75 mL) and the mixture was slowly allowed to warm to room temperature and stir for 18 h. The mixture was cooled to 0 °C and degassed, deionized water (15 mL) was added slowly. The mixture was allowed to slowly warm to room temperature and stir until the mixture was free-flowing. The mixture was filtered and washed with pentane (2 x 30 mL), and the combined filtrates were dried over MgSO$_4$ and concentrated by rotary evaporation to give a pale yellow liquid (5.08 g, 46.9 mmol, 78% yield), shown by ^{1}H NMR to be a mixture of regioisomers with some residual Et$_2$O and pentane. Used without further purification.

Synthesis of Li[$^{i\text{-}Pr}$Cp] (14): With cooling to –84 °C, *n*-BuLi (18.0 mL 2.5 M solution in hexanes, 45.0 mmol) was added to a solution of 5-(1-methylethyl)-1,3-cyclopentadiene (**13**, 4.86 g, 45.0 mmol) in Et$_2$O (45 mL) and the mixture was allowed to slowly warm to room temperature. Upon warming, the formation of copious white solid inhibited stirring. After sitting for 16 h, the solid was collected by vacuum filtration, washed with copious pentane, and dried in vacuo to give a white solid (4.67 g, 41.0 mmol, 91% yield) with a small quantity of pentane persisting even after extended drying. ^{1}H NMR (500 MHz, DMSO-*d*$_6$, δ): 5.17 (t, *J* = 2.4 Hz, 2H), 5.12 (t, *J* = 2.4 Hz, 2H), 2.72 (sept, *J* = 6.7 Hz, 1H), 1.07 (d, *J* = 6.7 Hz, 6H).

Synthesis of *n*-Bu$_3$Sn($^{i\text{-}Pr}$Cp) (15): The title compound was prepared according to a procedure adapted from the literature for the analogous compound *n*-Bu$_3$SnCp*.[23] *n*-Bu$_3$SnCl (6.0 mL, 22.1 mmol) was added to a mixture of Li[$^{i\text{-}Pr}$Cp] (**14**, 2.52 g, 22.1 mmol) in toluene (150 mL) and the mixture was stirred at room temperature for 3 days. A difficult filtration over Celite gave a yellow solution whose concentration gave a yellow oil (7.75 g, 19.5 mmol, 88% yield). ^{1}H NMR (500 MHz, CDCl3, δ): 6.21 (t, *J* = 1.6 Hz, 2H), 5.35 (t, *J* = 1.6 Hz, 2H), 2.77 (sept, *J* = 6.8 Hz, 1H), 1.46 (m, 6H), 1.29 (sext, *J* = 7.2 Hz, 6 H), 1.19 (d, *J* = 6.8 Hz, 6H), 0.89 (t, *J* = 7.2 Hz, 9H), 0.76 (m, 6H).

Synthesis of $^{i\text{-}Pr}$Cp$_2$TaCl$_2$ (16): The title compound was prepared according to a procedure adapted from the literature.[12a] *n*-Bu$_3$Sn($^{i\text{-}Pr}$Cp) (**15**, 7.75 g, 19.5 mmol) was added to a mixture of TaCl$_5$ (2.02 g, 5.63 mmol, freshly-sublimed) and dichloromethane (50 mL), giving a rapid color change from colorless to orange-red. The mixture was stirred for 7 days, during which it became a green-brown color. This mixture was concentrated to a volume of ~20 mL, layered with pentane, and chilled at –25 °C for 2 days. After this time a solid was collected by vacuum filtration, washed with pentane, and dried in vacuo to give a fine brown solid (1.99 g) that was used without further purification or characterization.

Synthesis of $^{i\text{-}Pr}$Cp$_2$TaH$_3$ (4): The title compound was prepared according to procedures adapted from the literature.[12a,b] Sodium bis(2-methoxyethoxy)aluminum hydride (2.9 mL 70 % w/w [~3.5 *M*] in toluene, 10.2 mmol) was added to a mixture of $^{i\text{-}Pr}$Cp$_2$TaCl$_2$ (**16**, 1.99 g, 4.3 mmol) in toluene (40 mL) and the solution was stirred 1 h. After this time it was cooled to 0 °C and degassed, deionized water (2.1 mL, 116.6 mmol) was added dropwise and the mixture was allowed to slowly warm to room temperature and stir until the viscous mixture became free-flowing. The red solution was separated from the precipitate and concentrated in vacuo to give a brown solid. Extraction into hexanes (65 mL) and cooling to –84 °C for 1 h gave an off-white solid that was collected and dried in vacuo (0.35 g, 0.89 mmol, 21% yield). ^{1}H NMR (500 MHz, C$_6$D$_6$, δ): 4.77 (t, *J* = 2.5 Hz, 4H), 4.69 (t, *J* = 2.5 Hz, 4H), 2.67 (sept, *J* = 6.7 Hz, 2H), 1.14 (d, *J* = 6.7 Hz, 12H), -1.06 (t, *J* = 10.2 Hz, 1H), -2.57 (d, *J* = 10.2 Hz, 2H); ^{13}C NMR (126 MHz, C$_6$D$_6$, δ): 121.7, 83.9, 83.8, 28.8, 24.5.

Synthesis of Li[$^{t\text{-}Bu}$Cp] (17): With cooling to 0 °C, MeLi (20.0 mL 1.6 *M* solution in Et$_2$O, 32.00 mmol) was added to a solution of 6,6'-dimethylfulvene (**12**, 4.53 g, 32.0 mmol) in Et$_2$O (150 mL) and allowed to slowly warm to room temperature and stirred 18 h, during which time a white solid formed and the bright yellow color faded. The white solid was collected by vacuum filtration, washed with copious pentane, and dried in vacuo to give a white solid (3.35, 26.2 mmol, 82% yield). ^{1}H NMR (500 MHz, DMSO-*d*$_6$, δ): 5.20 (t, *J* = 2.6 Hz, 2H), 5.10 (t, *J* = 2.6 H, 2H), 1.13 (s, 9H).

Synthesis of *n*-Bu$_3$Sn($^{t\text{-}Bu}$Cp) (18): The title compound was prepared according to a procedure adapted from the literature literature for the analogous compound *n*-Bu$_3$SnCp*.[23] *n*-Bu$_3$SnCl (6.0 mL, 22.1 mmol) was added to a mixture of Li[$^{t\text{-}Bu}$Cp] (**17**, 2.83 g, 22.1 mmol) in toluene (175 mL) and the mixture was stirred at room temperature overnight. After this time the mixture was filtered over Celite, washed with toluene, and the combined filtrates were concentrated in vacuo to give a yellow oil (7.97 g, 19.4 mmol, 88% yield). ^{1}H NMR (500 MHz, CDCl$_3$, δ): 6.35 (t, *J* = 1.6 Hz, 2H), 5.25 (t, *J* = 1.6 Hz, 2H), 1.46 (m, 6H), 1.30 (sext, *J* = 7.2 Hz, 6 H), 1.22 (s, 9H), 0.89 (t, *J* = 7.2 Hz, 9H), 0.76 (m, 6H).

Synthesis of $^{t\text{-}Bu}$Cp$_2$TaCl$_2$ (19): The title compound was prepared according to a procedure adapted from the literature for the

analogous compound $^{i\text{-}Pr}Cp_2TaCl_2$[12a] *n*-$Bu_3Sn(^{t\text{-}Bu}Cp)$ (**18**, 7.97 g, 19.38 mmol) was added to a mixture of $TaCl_5$ (2.00 g, 5.6 mmol, freshly-sublimed) in dichloromethane (50 mL), giving a rapid color change from colorless to deep red. The mixture was stirred at room temperature for 7 days, during which it became a deep green color. This mixture was concentrated to a volume of ~20 mL, layered with pentane, and chilled at –25 °C for 1 day. After this time a solid was collected by vacuum filtration, washed with pentane, and dried in vacuo to give a fine brown solid (1.73 g) that was used without further purification or characterization.

Synthesis of $^{t\text{-}Bu}Cp_2TaH_3$ (5): The title compound was prepared according to procedures adapted from the literature for the analogous compound $^{i\text{-}Pr}Cp_2TaH_3$.[12a,b] Sodium bis(2-methoxyethoxy)aluminum hydride (2.4 mL 70 % w/w [~3.5 M] in toluene, 8.4 mmol) was added to a mixture of $^{t\text{-}Bu}Cp_2TaCl_2$ (**19**, 1.73 g, 3.5 mmol) in toluene (35 mL), and the solution was stirred for 1 h. After this time it was cooled to 0 °C, and degassed, deionized water (1.7 mL, 94.4 mmol) was added dropwise and the mixture was allowed to slowly warm to room temperature and stirred until the viscous mixture became free-flowing. The orange solution was separated from the precipitate and concentrated in vacuo to give an orange solid. Extraction into pentane (25 ml) and cooling to –84 °C for 1 h gave a white microcrystalline solid that was collected and dried in vacuo (0.27 g, 0.64 mmol, 18% yield). ^{1}H NMR (500 MHz, C_6D_6, δ): 4.73 (t, *J* = 2.5 Hz, 4H), 4.63 (t, *J* = 2.5 Hz, 4H), 1.26 (s, 18H), -1.37 (t, *J* = 9.8 Hz, 1H), -2.78 (d, *J* = 9.8 Hz, 2H); ^{13}C NMR (126 MHz, C_6D_6, δ): 83.0, 82.1, 31.9, 30.6.

COMPUTATIONAL SECTION

Calculations were performed with Gaussian 16.[24] An ultrafine integration grid and the keyword 5d were used for all calculations. Except when evaluating other methods as specified in the Supporting Information, geometry optimizations of the stationary points were carried out in the gas phase with the M06L[25] functional with BS1 (BS1 = the LANL2DZ pseudopotential/basis set for Ta and the 6-31+G(d,p) basis set for all other atoms). Frequency analyses were carried out at the same level to evaluate the zero-point vibrational energy and thermal corrections. The nature of the stationary points was determined in each case according to the appropriate number of negative eigenvalues of the Hessian matrix. Forward and reverse intrinsic reaction coordinate calculations were carried out on the optimized transition structures to ensure that they indeed connect the appropriate reactants and products.[26] Multiple conformations and configurations were considered for all structures, and the lowest energy structures are reported. Unless otherwise specified in the Supporting Information, single point energy calculations were performed with the M06[27] functional with BS2 (BS2 = the SDD pseudopotential/basis set for Ta and the 6-311++G(2d,p) basis set for all other atoms). Bulk solvent effects were considered implicitly in the single point energy calculations through the CPCM solvation model.[28] All thermochemical quantities were computed with the GoodVibes code (373.15 K).[18] Bond lengths were measured using Gaussview 5.0.[29] 3D images of structures were prepared with Cylview.[30]

ASSOCIATED CONTENT

Supporting Information

The Supporting Information is available free of charge on the ACS Publications website.

NMR spectra, rate data, computational details, and energies of calculated structures (PDF)

Cartesian coordinates of calculated structures (xyz)

Notes

The authors declare no competing financial interests.

AUTHOR INFORMATION

Corresponding Author

* Email: sharon.neufeldt@montana.edu

ORCID

Sharon R. Neufeldt: 0000-0001-7995-3995; Steven M. Rehbein: 0000-0002-9240-1260; Matthew J. Kania: 0000-0003-4445-9780.

ACKNOWLEDGMENT

Acknowledgment is made to the donors of The American Chemical Society Petroleum Research Fund (57849-DNI3) and to Montana State University for support of this research. Calculations were performed on Expanse at SDSC and Bridges-2 at the Pittsburgh Supercomputing Center through XSEDE/ACCESS (CHE170089), which is supported by NSF (ACI-1548562), as well as on the Hyalite High Performance Computing System at MSU. Support for MSU's NMR Center was provided by the NSF (MRI:CHE-2018388 and MRI:DBI-1532078), MSU, and the Murdock Charitable Trust Foundation (2015066:MNL). The authors thank Brian Tripet, Michael Mock, and Nicholas Stadie for helpful discussions, and the MSU NMR Core Facility for their expertise.

REFERENCES

1. Selected reviews: (a) Parshall, G. W. Homogeneous Catalytic Activation of C—H Bonds. *Acc. Chem. Res.* **1975**, *8*, 113-117; (b) Rothwell, I. P. Carbon-Hydrogen Bond Activation in Early Transition Metal Systems. *Polyhedron* **1985**, *4*, 177-200; (c) Stahl, S. S.; Labinger, J. A.; Bercaw, J. E. Homogeneous Oxidation of Alkanes by Electrophilic Late Transition Metals. *Angew. Chem., Int. Ed*. **1998**, *37*, 2180–2192; (d) Crabtree, R.H. Alkane C–H activation and functionalization with homogeneous transition metal catalysts: a century of progress—a new millennium in prospect. *J. Chem. Soc, Dalton Trans.* **2001**, 2437-2450; (e) Labinger, J. A.; Bercaw, J. E. Understanding and exploiting C—H bond activation. *Nature* **2002**, *417*, 507-514; (f) Lersch, M.; Tilset, M. Mechanistic Aspects of C–H Activation by Pt Complexes. *Chem. Rev*. **2005**, *105*, 2471–2526; (g) Hartwig, J. F. Evolution of C–H Bond Functionalization from Methane to Methodology *J. Am. Chem. Soc.* **2016**, *138*, 2–24; (h) Gunsalas, N.J.; Koppaka, A.; Park, S.H.; Bischof, S.M.; Hashiguchi, B.G.; Periana, R.A. Homogeneous functionalization of methane. *Chem. Rev.* **2017**, *117*, 8521-8573.

2. Kepp, K.P. A quantitative scale of oxophilicity and thiophilicity. *Inorg. Chem.* **2016**, *55*, 9461-9470.

3. Beaumier, E.P.; Pearce, A.J.; See, X.Y.; Tonks, I.A., Modern applications of low-valent early transition metals in synthesis and catalysis, *Nat. Chem. Rev.* **2019**, *3*, 15-34.

4. Waterman, R. σ-Bond metathesis: a 30-year retrospective. *Organometallics* **2013**, *32*, 7249–7263.

5. Seminal examples that are not believed to proceed through oxidative addition (a) Chamberlain, L.; Keddington, J.; Rothwell, I. P. The chemistry of sterically crowded aryl-oxide ligands. Part 2. Cyclotantalation of 2,6-di-*tert*-butylphenoxide. *Organometallics* **1982**, *1*, 1538-1540; (b) Chamberlain, L.; Rothwell, A. P.; Rothwell, I. P. Photochemical α-Hydride Abstraction. *J. Am. Chem. Soc.* **1984**, *106*, 1847-1848.

6. Examples that are likely to proceed through oxidative addition: (a) Nugent, W. A.; Ovenall, D. W.; Holmes, S. J. Catalytic C-H activation in early transition-metal dialkylamides and alkoxides. *Organometallics* **1983**, *2*, 161-162; (b) LaPointe, R. E.; Wolczanski, P. T.; Mitchell, J. F. Carbon Monoxide Cleavage by $(silox)_3Ta$ (silox = t-Bu_3SiO^-). *J. Am. Chem. Soc.* **1986**, *108*, 6382-6384; (c) Steffey, B. D.; Chamberlain, L. R.; Chesnut, R. W.; Chebi, D. E.; Fanwick, P. E.; Rothwell, I. P. Intramolecular activation of aliphatic and aromatic carbon-hydrogen bonds by tantalum(III) metal centers: synthesis and structure of the bis-metalated compounds $Ta(OC_6H_3Bu^tCMe_2CH_2)_2Cl$ and $Ta(OC_6H_3PhC_6H_4)_2$ (OAr-2,6-Ph_2) (OAr-2,6-Ph_2=2,6-diphenylphenoxide). *Organometallics* **1989**, *8*, 1419-1423. (d) Yu, J. S.; Fanwick, P. E.; Rothwell, I. P. Intramolecular Alkane Dehydrogenation and Functionalization at Niobium Metal Centers. *J. Am. Chem. Soc.* **1990**, *112*, 8171-8172. (e) Yu, J. S.; Felter, L.; Potyen, M. C.; Clark, J. R.; Visciglio, V. M.; Fanwick, P. E.; Rothwell, I. P. Intramolecular Dehydrogenation of Alkyl Groups at Niobium Aryloxide Centers: Bonding and Reactivity of the Ensuing Niobacyclopropane Ring. *Organometallics* **1996**, *15*, 4443-4449; (f) Riley, P. N.; Clark, J. R.; Fanwick, P. E.; Rothwell, I. P. Synthesis and structure of niobium and tantalum derivatives of bis(dicyclohexylphosphino)methane (dcpm). *Inorg. Chim. Acta* **1999**, *288*, 35-39; (g) Rankin, M.; Cummins, C. C. Carbon Dioxide Reduction by Terminal Tantalum Hydrides: Formation and Isolation of Bridging Methylene Diolate Complexes. *J. Am. Chem. Soc.* **2010**, *132*, 10221-10223. (h) Kriegel, B. M.; Bergman, R. G.; Arnold, J. Generation of low-valent tantalum species by reversible C–H activation in a cyclometallated tantalum hydride complex. *Dalton Trans.* **2014**, *43*, 10046-10056.

7. (a) Watson, P. Methane Exchange Reactions of Lanthanide and Early-Transition-Metal Methyl Complexes. *J. Am. Chem. Soc.* **1983**, *105*, 6491-6493l (b) Tsang, J. Y. K., Buschhaus, M. S. A. & Legzdins, P. Selective activation and functionalization of linear alkanes initiated under ambient conditions by a tungsten allyl nitrosyl complex. *J. Am. Chem. Soc*. **2007**, *129*, 5372–5373; (c) Baillie, R. A.; Man, R. W. Y.; Shree, M. V.; Chow, C.; Thibault, M. E.; McNeil, W. S.; Legzdins, P. Intermolecular C–H Activations of Hydrocarbons Initiated by Cp*M(NO)(CH2CMe3)(η3-CH2CHCHPh) Complexes (M = Mo, W). *Organometallics* **2011**, *30*, 6201–6217.

8. Alkane activation at silica-supported tantalum complexes has also been reported, with evidence for a σ-bond metathesis mechanism: (a) Vidal, V.; Théolier, A.; Thivolle-Cazat, J.; Basset, J.-M. Metathesis of Alkanes Catalyzed by Silica-Supported Transition Metal Hydrides. *Science* **1997**, *276*, 99–102. (b) Thieuleux, C.; Copéret, C.; Dufaud, V.; Marangelli, C.; Kuntz, E.; Basset, J.-M. Heterogeneous well-defined catalysts for metathesis of inert and not so inert bonds. *J. Mol. Catal. A: Chem.* **2004**, *213*, 47–57. (c) Basset, J. M.; Copéret, C.; Lefort, L.; Maunders, B. M.; Maury, O.; Le Roux, E.; Saggio, G.; Soignier, S.; Soulivong, D.; Sunley, G. J.; Taoufik, M.; Thivolle-Cazat, J. Primary Products and Mechanistic Considerations in Alkane Metathesis. *J. Am. Chem. Soc.* **2005**, *127*, 8604–8605. (d) Le Roux, E.; Taoufik, M.; Copéret, C.; de Mallmann, A.; Thivolle-Cazat, J.; Basset, J.-M.; Maunders, B. M.; Sunley, G. J. Development of Tungsten-Based Heterogeneous Alkane Metathesis Catalysts Through a Structure– Activity Relationship. *Angew. Chem., Int. Ed.* **2005**, *44*, 6755–6758. (e) Chen, Y.; Edy, A.; Ali, H.; Bilel, H.; Lyndon, E.; Basset, J. M. Alkane Metathesis with the Tantalum Methylidene $[(\equiv SiO)Ta(:CH_2)Me_2]$/$[(\equiv SiO)_2Ta(:CH_2)Me]$ Generated from Well-Defined Surface Organometallic Complex $[(\equiv SiO)Ta^VMe_4]$. *J. Am. Chem. Soc.* **2015**, *137*, 588–591. (f) Soulivong, D.; Norsic, S.; Taoufik, M.; Copéret, C.; Thivolle- Cazat, J.; Chakka, S.; Basset, J.-M. Non-Oxidative Coupling Reaction of Methane to Ethane and Hydrogen Catalyzed by the Silica- Supported Tantalum Hydride: $(SiO)_2Ta$-H. *J. Am. Chem. Soc.* **2008**, *130*, 5044–5045. (g) Pasha, F. A.; Cavallo, L.; Basset, J. M. Mechanism of n-Butane Hydrogenolysis Promoted by Ta-Hydrides Supported on Silica. *ACS Catal.* **2014**, *4*, 1868–1874.

9. (a) Flores, J. A.; Cavaliere, V. N.; Buck, D.; Pintér, B.; Chen, G.; Crestani, M. G.; Baik, M.-H.; Mindiola, D. J. Methane activation and exchange by titanium-carbon multiple bonds. *Chem. Sci.* **2011**, *2*, 1457-1462; (b) Solowey, D. P.; Mane, M. V.; Kurogi, T.; Carroll, P. J.; Manor, B. C.; Baik, M.-H.; Mindiola, D. J. A new and selective cycle for dehydrogenation of linear and cyclic alkanes under mild conditions using a base metal. *Nature. Chem.* **2017**, *9*, 1126-1132; (c) Kurogi, T.; Won, J.; Park, B.; Trofymchuk, O. S.; Carroll, P. J.; Baik, M.-H.; Mindiola, D. J. Room temperature olefination of methane with titanium–carbon multiple bonds. *Chem. Sci.* **2018**, *9*, 3376-3385.

10. For examples of studies on the microscopic reverse of $C_{(sp3)}$—H oxidative addition, reductive elimination, see: (a) Churchill, D. G.; Janak, K. E.; Wittenberg, J. S.; Parkin, G. Normal and Inverse Primary Kinetic Deuterium Isotope Effects for C-H Bond Reductive Elimination and Oxidative Addition Reactions of Molybdenocene and Tungstenocene Complexes: Evidence for Benzene σ-Complex Intermediates. *J. Am. Chem. Soc.* **2003**, *125*, 1403-1420; (b) Parkin, G. Temperature-Dependent Transitions Between Normal and Inverse Isotope Effects Pertaining to the Interaction of H–H and C–H Bonds with Transition Metal Centers. *Acc. Chem. Res.* **2009**, *42*, 315–325.

11. Rehbein, S. M.; Kania, M. J.; Neufeldt, S. R. Experimental and Computational Evaluation of Tantalocene Hydrides for C—H Activation of Arenes. *Organometallics* **2021**, *40*, 2666-2677.

12. (a) Green, M.L.H. & Jousseaume, B. Bis(η-isopropylcyclopentadienyl)tantalum chemistry: some hydride, carbonyl, alkyl, alkyne and tertiaryphosphine derivatives, and an improved synthesis of dichlorobiscyclopentadienylniobium. *J. Organomet. Chem*. **1980**, *193*, 339-344; (b) Leblanc, J.-C.; Reynoud, J.-F.; Moise, C. Complexes bis cyclopentadienyles substitues du tantale: synthese et reactivite de dichlorures, de tri- et de monohydrures. *C. R. Acad. Sc. Paris* **1982**, *295*, 755-757; (c) Schmidt, S.; Sundermeyer, J. Höhervalente derivate der d-metall-säuren X. Imidokomplexe des fünf- und vierwertigen niobs und tantals mit halbsandwich- und metallocenstruktur *J. Organomet. Chem*. **1994**, *472*, 127-138; (d) Korolev, A.V.; Rheingold, A.L.; Williams, D.W. A General Route to Labile Niobium and Tantalum d^0 Monoimides. Discussion of Metal-Nitrogen Vibrational Modes. *Inorg. Chem*. **1997**, *36,* 2647-2655; (e) Findlay, A.E.; Leelasubcharoen, S.; Kuzmina, L.G.; Howard, J.A.K.; Nikonov, G.I. Phosphido-bridged Ta/Rh bimetallic complex: synthesis, structure, and catalytic hydrosilylation of acetophenone. *Dalton Trans.* **2010**, *39*, 9264-9269.

13. For an overview of the structure and geometry of bent metallocenes, see (a) Lauher, J. W.; Hoffman, R. Structure and chemistry of bis(cyclopentadienyl)-MLn complexes. *J. Am. Chem. Soc.* **1976**, *98*, 1729-1742; (b) Green, J. C. Bent metallocenes revisited. *Chem. Soc. Rev.* **1998**, *27*, 263-271.

14. (a) Barefield, E. K.; Parshall, G. W.; Tebbe, F. N. Catalysis of Aromatic Hydrogen-Deuterium Exchange by Metal Hydrides. *J. Am. Chem. Soc.* **1970**, *92*, 5234–5235. (b) Parshall, G. W. Intramolecular aromatic substitution in transition metal complexes. *Acc. Chem. Res*. **1970**, *3*, 139–144. (c) Parshall, G. W.; Tebbe, F. N. Hydride Derivatives of Niobocene and Tantalocene. *J. Am. Chem. Soc*. **1971**, *93*, 3793–3795. (d) Klabunde, U.; Parshall, G. W. Activation of Aromatic Carbon-Hydrogen Bonds by Transition Metal Complexes. II. Substituted Benzenes. *J. Am. Chem. Soc.* **1972**, *94*, 9081–9087. (e) Foust, D. F.; Rogers, R. D.; Rausch, M. D.; Atwood, J. L. Photoinduced Reactions of $(\eta^5\text{-}C_5H_5)_2M(CO)H$ (M = Nb, Ta) and the Molecular Structure of $(\eta^5\text{-}C_5H_5)_2Ta(CO)H$. *J. Am. Chem. Soc.* **1982**, *104*, 5646–5650.

15. Selected examples of C(sp2)—H activation at other metallocene hydrides: (a) Giannotti, C.; Green, M. L. H. Photo-induced

insertion of bis-π-cyclopentadienyltungsten into aromatic carbon–hydrogen bonds. *J. Chem. Soc., Chem. Commun.* **1972**, 1114b-1115; (b) Geoffrey, G. L.; Bradley, M. G. Photochemistry of Transition Metal Hydride Complexes. 3. Photoinduced Elimination of Molecular Hydrogen from $[Mo(\eta^5\text{-}C_5H_5)_2H_2]$ *Inorg. Chem.* **1978**, *17*, 2410-2414.

16. Thermal decomposition of Cp_2TaH_3 can lead to a tantalum monohydride dimer; see 13a.

17. For example, the Mo analogue of **1** ($Cp_2MoH_3^+$) undergoes thermally activated exchange of the lateral and central hydrides even at room temperature, such that a ^1H NMR spectrum of this complex taken at room temperature shows only a single hydride resonance: Heinekey, D. M. Exchange Coupling in Metallocene Trihydride Complexes. *J. Am. Chem. Soc.* **1991**, *113*, 6074-6077.

18. Luchini, G.; Alegre-Requena, J. V.; Funes-Ardoiz, I.; and Paton, R. S. GoodVibes: Automated Thermochemistry for Heterogeneous Computational Chemistry Data, *F1000Research*, **2020**, *9*, 291.

19. Seminal examples using the term "tuck-in": (a) Bercaw, J. E.; Marvich, R. H.; Bell, L. G.; Brintzinger, H. H. Titanocene as an Intermediate in Reactions Involving Molecular Hydrogen and Nitrogen. *J. Am. Chem. Soc.* **1972**, *94*, 1219-1238; (b) Martin, H. A.; Van Gorkom, M.; De Jongh, R. O. Directive Effect of a Methyl Substituent in the Exchange Reaction of Ring Hydrogen with Molecular Deuterium in Dicyclopentadienyltitanium Complexes. *J. Organomet. Chem.* **1972**, *36*, 93-100; (c) Carter, S. T.; Clegg, W.; Gibson, V. C.; Kee, T. P.; Sanner, R. D. A Double Intramolecular Ring Metalation: Formation, Spectroscopic Characterization, and Molecular Structure of $(C_5Me_3(CH_2)_2)Ta(H)_2(PMe_3)_2$. *Organometallics* **1989**, *8*, 253-255.

20. Brunner, H.; Wachter, J.; Gehart, G. Leblanc, J.-C.; Moïse, C. Preparation and Reactivity of Peralkylated Tantalocene Sulfur Complexes Having a Fulvenoid Substructure. *Organometallics* **1996**, *15*, 1327-1330.

21. Willans, M. J.; Schurko, R. W. A Solid-State NMR and ab Initio Study of Sodium Metallocenes. *J. Phys. Chem. B* **2003**, *107*, 5144–5161.

22. Coşkun, N. and Erden, I., An efficient catalytic method for fulvene synthesis. Tetrahedron, 2011, 67, 8607-8614.

23. Sanner, R.D.; Carter, S.T.; Bruton, Jr., W.J. The preparation of mono(η5-pentamethylcyclopentadienyl) compounds of tantalum(V). J. Organomet. Chem. 1982, 240, 157-162.

24. Frisch, M. J.; Trucks, G. W.; Schlegel, H. B.; Scuseria, G. E.; Robb, M. A.; Cheeseman, J. R.; Scalmani G., Barone, V.; Petersson, G. A.; Nakatsuji, H.; Li, X.; Caricato, M.; Marenich, A. V.; Bloino, J.; Janesko, B. G.; Gomperts, R.; Mennucci, B.; Hratchian, H. P.; Ortiz, J. V.; Izmaylov, A. F.; Sonnenberg, J. L.; Williams-Young, D.; Ding, F.; Lipparini, F.; Egidi, F.; Goings, J.; Peng, B.; Petrone, A.; Henderson, T.; Ranasinghe, D.; Zakrzewski, V. G.; Gao, J.; Rega, N.; Zheng, G.; Liang, W.; Hada, M.; Ehara, M.; Toyota, K.; Fukuda, R.; Hasegawa, J.; Ishida, M.; Nakajima, T.; Honda, Y.; Kitao, O.; Nakai, H.; Vreven, T.; Throssell, K.; Montgomery, J. A. Jr.; Peralta, J. E.; Ogliaro, F.; Bearpark, M. J.; Heyd, J. J.; Brothers, E. N.; Kudin, K. N.; Staroverov, V. N.; Keith, T. A.; Kobayashi, R.; Normand, J.; Raghavachari, K.; Rendell, A. P.; Burant, J. C.; Iyengar, S. S.; Tomasi, J.; Cossi, M.; Millam, J. M.; Klene, M.; Adamo, C.; Cammi, R.; Ochterski, J. W.; Martin, R. L.; Morokuma, K.; Farkas, O.; Foresman, J. B.; and Fox, D. J. *Gaussian 16*; Gaussian, Inc., Wallingford CT, 2016.

25. Zhao, Y.; Truhlar, D. G. A New Local Density Functional for Main-Group Thermochemistry, Transition Metal Bonding, Thermo-chemical Kinetics, and Noncovalent Interactions. *J. Chem. Phys.* **2006**, *125*, 194101.

26. (a) Gonzalez, C.; Schlegel, H. B. An Improved Algorithm for Reaction Path Following. *J. Chem. Phys.* **1989**, *90*, 2154–2161; (b) Gonzalez, C.; Schlegel, H. B. Reaction Path Following in Mass-Weighted Internal Coordinates. *J. Phys. Chem.* **1990**, *94*, 5523–5527; (c) Fukui, K. The Path of Chemical Reactions - the IRC Approach. *Acc. Chem. Res.* **1981**, *14*, 363–368

27. Zhao, Y.;Truhlar, D. G. The M06 suite of density functionals for main group thermochemistry, thermochemical kinetics, noncovalent interactions, excited states, and transition elements: two new functionals and systematic testing of four M06-class functionals and 12 other functionals. *Theor. Chem. Acc.,* **2008**, *120,* 215–241.

28. Cossi, M.; Rega, N.; Scalmani, G.; Barone, V. Energies, structures, and electronic properties of molecules in solution with the C-PCM solvation model. *J. Comput. Chem.* **2003**, *24*, 669–681.

29. GaussView, Version 6, Dennington, Roy; Keith, Todd A.; Millam, John M. Semichem Inc., Shawnee Mission, KS, 2016.

30. Legault, C. Y. *CYLview, 1.0b*; Universitéde Sherbrooke, 2009 http://www.cylview.org.

TOC Graphic: